ChemComm

RSC Publishing

COMMUNICATION

View Article Online
View Journal | View Issue

Cite this: *Chem. Commun.*, 2013, **49**, 2192

Received 5th November 2012,
Accepted 30th January 2013

DOI: 10.1039/c3cc38009b

www.rsc.org/chemcomm

Carbon with hierarchical pores from carbonized metal–organic frameworks for lithium sulphur batteries†

Kai Xi,‡ Shuai Cao,‡ Xiaoyu Peng, Caterina Ducati, R. Vasant Kumar* and Anthony K. Cheetham*

This paper presents a novel method and rationale for utilizing carbonized MOFs for sulphur loading to fabricate cathode structures for lithium–sulphur batteries. Unique carbon materials with differing hierarchical pore structures were synthesized from four types of zinc-containing metal–organic frameworks (MOFs). It is found that cathode materials made from MOFs-derived carbons with higher mesopore (2–50 nm) volumes exhibit increased initial discharge capacities, whereas carbons with higher micropore (<2 nm) volumes lead to cathode materials with better cycle stability.

In this work we have explored the possibility of using porous carbon scaffolds, produced by carbonizing zinc-containing metal–organic framework (MOF) materials,[1] as suitable electrically conducting hosts for encapsulating sulphur in a Li–S battery (Fig. 1). High temperature pyrolysis of MOFs is shown to produce carbons with tunable hierarchical porous morphologies (SI-3, ESI†). We have selected 4 different MOFs, all based on zinc metal centres because zinc can be readily eliminated as metallic vapour during high temperature pyrolysis;[2] this approach eliminates the additional step of separating any remaining metal oxide from the carbon. Unlike inorganic precursors, the presence of organic ligands in MOFs eliminates the need for an additional carbon source,[3] and it is possible to produce variations in the pore volume, surface area and pore size distribution in the resulting carbon structures, which can then serve as hosts for sulphur loading to make Li–S batteries.

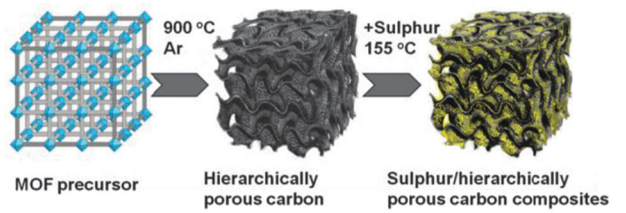

Fig. 1 Scheme of sulphur–hierarchical porous carbon composite preparation.

A lithium–sulphur battery has a high theoretical capacity of 1675 mA h g^{-1} of elemental sulphur and a high nominal theoretical energy density of 2600 W h kg^{-1} of cell weight.[4–6] It has the potential to offer a practical energy density upgrade in comparison with the present lithium-ion batteries (150 W h kg^{-1}).[7] Furthermore, elemental sulphur has advantages of being low cost, available in abundance both naturally and as an industrial by-product, and being environmentally friendly.[6]

Despite its considerable advantages, the lithium–sulphur battery is plagued with problems arising from the highly insulating nature of sulphur (5×10^{-30} S cm^{-1} at 25 °C) and the high solubility of lithium polysulphides in the organic electrolyte. The cycle life of a Li–S battery is generally poor due to redox shuttle mechanisms[8] from excessive dissolution and migration of polysulphides which must be controlled. In these efforts, the inclusion of a porous matrix based on carbon,[9–12] polymer,[13] silica[14,15] or MOF[14] has shown a marked increase in the capacity retention arising from their strong nanoporous adsorption capability. Among them, porous carbon materials are particularly attractive due to their excellent conductivity and inherently large surface area.

Recently, there has been growing research interest for producing porous carbon by direct carbonization of MOFs for a variety of potential applications.[2,16,17] The carbonized products exhibit micro- (<2 nm), meso- (2–50 nm), and macropores (>50 nm) with exceptionally high specific surface areas and high pore volumes. The following four sacrificial MOFs sources were selected in this work: zeolitic imidazolate framework-8[18] (ZIF-8), room temperature synthesized metal–organic framework-5[19] (RT-MOF-5), solvothermally synthesized MOF-5[20] (solvo-MOF-5), and $[Zn_3(fumarate)_3(dmf)_2]$ (ZnFumarate) (SI-2, ESI†).[16] All the selected MOFs are crystalline compounds containing Zn ions co-ordinated to rigid organic ligands. ZIF-8 and MOF-5 were chosen as prototypical MOFs, while pyrolysis of ZnFumarate has been shown to produce hierarchical carbon with exceptional porosity.[16] These MOF precursors were pyrolyzed under Ar atmosphere to produce hierarchical carbons.[2,16,17] The resulting porous

Department of Materials Science and Metallurgy, University of Cambridge, Cambridge, CB2 3QZ, UK. E-mail: rvk10@cam.ac.uk, akc30@cam.ac.uk; Tel: +44 (0)1223 334327, +44 (0)1223 767061

† Electronic supplementary information (ESI) available. See DOI: 10.1039/c3cc38009b

‡ These authors contributed equally to this work.

carbons were characterized by powder X-ray diffraction (PXRD), Raman spectroscopy, scanning electron microscopy (SEM), energy dispersive X-ray spectroscopy (EDS), transmission electron microscope (TEM) and N_2 sorption measurements (SI-5, ESI†).

For loading the pyrolyzed carbon with sulphur, a thermal process has been used whereby up to 55 wt% sulphur is infiltrated into the porous carbon host matrix (SI-4, ESI†). The sulphur composite cathode was prepared by compressing the mixture of sulphur and the porous carbon, with carbon black and a polytetrafluoroethylene (PTFE) binder in a weight ratio of 70 : 20 : 10. Two of the un-pyrolyzed Zn-MOF precursors (ZIF-8 and RT-MOF-5) were also tested as scaffold materials and the results compared with the pyrolyzed materials. The cells were tested using a galvanostatic charge–discharge method at room temperature at a specific current of 400 mA g^{-1} in the electrolyte ($LiN(CF_3SO_2)_2$/DOL : DME = 1 : 1 (v/v)) to evaluate the electrochemical capacity and cycle life (SI-6, ESI†).

The PXRD patterns (Fig. S1, ESI†) show that all starting MOFs are highly crystalline prior to carbonization. Their transformation into amorphous carbonaceous materials after pyrolysis was confirmed by PXRD by the loss of sharp Bragg reflections. (Fig. S2, ESI†) As in previous studies, Raman spectra reveal that the carbonized MOFs are composed of both graphitic and disordered carbon atoms.[2,17] (Fig. S7, ESI†) SEM images have shown that the resulting carbons, while being amorphous, still manage to retain the basic crystalline facetted shapes of the MOF precursors to some extent. (Fig. S4, ESI†) TEM observations were carried out to further examine the morphologies of the amorphous porous carbons (Fig. 2 and Fig. S3, ESI†). As shown in Fig. S3a and b (ESI†), carbon from ZIF-8 exhibits micron-sized particles with a relatively uniform porous structure with small pore sizes normally less than 2 nm. Carbon from RT-MOF-5 (Fig. 2a and Fig. S4f, ESI†) shows smaller agglomerated particles than carbon from solvo-MOF-5 (Fig. S3c and S4d, ESI†). The two kinds of pyrolyzed MOF-5 samples both show polyhedron-like morphologies with highly developed porous structure with a homogeneous micropore size distribution (Fig. 2c and Fig. S3d, ESI†). Furthermore, carbon from RT-MOF-5 presents a highly interconnected 3D micro- and mesopore network that extends throughout the carbon monolith. (Fig. 2) Carbon from solvo-MOF-5 shows irregular macropores in the micron-sized cubes, (Fig. S3c and S4d, ESI†) while carbon derived from ZnFumarate formed as platelets with widths in the range of hundreds nm with rather disordered graphitic micropores. (Fig. S3e and f, ESI†) Textural characterizations by N_2 sorption measurements (Fig. 2d and Fig. S5, ESI†) corroborate the above TEM findings. As illustrated in Table 1, the pores in carbon from ZIF-8 are composed almost entirely of micropores (97.5%), confirming the absence of significant meso- or macropores. The carbons from RT-MOF-5 and from solvo-MOF-5 show quite different porous structures; carbon from RT-MOF-5 consists of a higher total pore volume at 1.92 cm^3 g^{-1} with a rather low micropore proportion of 16.1%, while in carbon from solvo-MOF-5 the micropores make up 61.9% of the total pore volume. Meanwhile, the carbon from ZnFumarate demonstrates the most porous carbon with a pore volume totaling up to 3.99 cm^3 g^{-1} and a modest amount (31.8%) of micropores. Since ZnFumarate has the highest Zn content among the MOF precursors, the large pore volume corroborates the finding that the porosity of the carbon materials depends linearly on the Zn/C ratio of the MOF precursors.[16] After sulphur loading, the surface area of the sulphur–carbon composite is reduced substantially. (Fig. S8, ESI†) These variations in textural characteristics were further studied to reveal the underlying relationship between the porous carbon textures and the Li–S battery capacities/cycle stabilities.

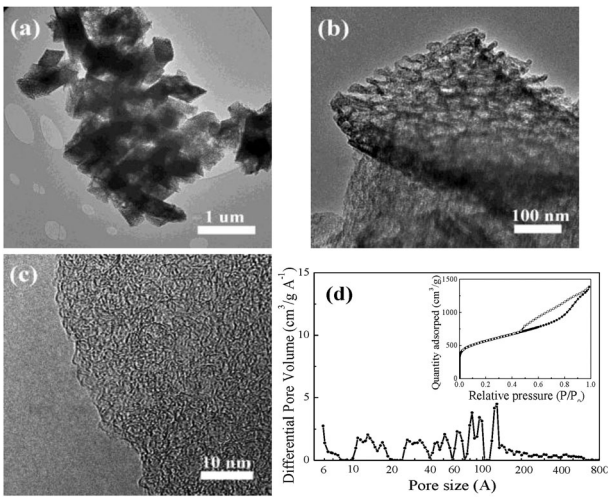

Fig. 2 TEM images of hierarchical porous carbon from RT-MOF-5 (a–c), and N_2 adsorption–desorption isotherms of the sample (adsorption: ●; desorption: ○), and their corresponding pore size distribution (d).

Both the thermal decomposition of the MOFs and the transformation to porous carbons take place simultaneously during pyrolysis. Loss of zinc and other non-carbon components of the MOFs by vaporisation plays a crucial role in the structural reorganization of MOF into hierarchically porous carbon, giving rise to micro-, meso-, and macropores. According to the EDS spectrum (Fig. S9, ESI†), there is no Zn present in carbonized MOFs except in pyrolyzed ZIF-8, which could be attributed to residual ZnO. The first discharge curves for a Li–S cell are shown in Fig. 3a and Fig. S6a (ESI†). Initial capacities of 542.1 and 919.4 mA h g^{-1} are observed for the non-carbonized sulphur–ZIF-8 and sulphur–RT-MOF-5 composites, respectively. Theoretically, there are two potential regions, one sloping down from 2.4–2.1 V and a second one as a plateau at 2.1 V (*vs.* Li/Li^+); these correspond to the formation of long-chain soluble lithium polysulfides (Li_2S_n; where n is typically 4–8) and short-chain solid sulphides (Li_2S_2 and Li_2S), respectively.[8] The plateau is lower than 2.1 V, mainly due to the high ohmic polarization with these MOF composites, and the capacities drop off rapidly with cycling, most likely due to the poor conductivity of the scaffolds and the tendency of sulphur to bond with zinc in the scaffold. On using the carbonized material as scaffolds in the cathode, the initial discharge capacities increase to values in the range 919.4 to 1471.8 mA h g^{-1}, with most of the increase arising from the 2.1 V plateaus.

The cycle performance of the cells is illustrated in Fig. 3b and Fig. S6b (ESI†). The amount of total pores correlates with sulphur loading. Micropores (<2 nm) help improve cycle life[11] by effectively confining polysulfide anion diffusion in the

Table 1 Textural characteristics of porous carbon from MOFs

Samples of carbon derived from	BET surface area ($m^2\ g^{-1}$)	Total pore volume[a] ($cm^3\ g^{-1}$)	Micropore volume ($cm^3\ g^{-1}$)	Mesopore volume ($cm^3\ g^{-1}$)	Macropore volume ($cm^3\ g^{-1}$)	Surface area of MOFs ($m^2\ g^{-1}$)
ZIF-8	969	0.40	0.39	0	0	1630[18]
RT-MOF-5	1945	1.92	0.31	1.41	0.03	3909[19]
Solvo-MOF-5	2372	1.26	0.78	0.30	0.13	2900[20]
ZnFumarate	4793	3.99	1.27	2.24	0.22	35.6

[a] Pores with dimensions up to 999 Å by NLDFT, assuming carbon slit pore geometry.

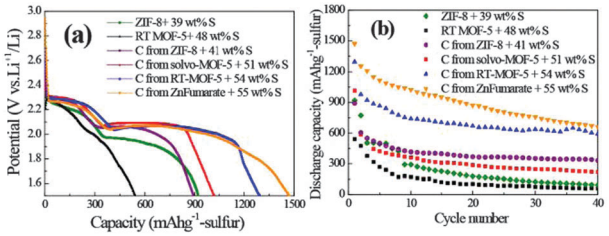

Fig. 3 The first discharge curves (a) and cycle performance (b) of samples at specific current of 400 mA g^{-1} between 1.5 and 3.0 V (*vs.* Li^+/Li) in the electrolyte ($LiN(CF_3SO_2)_2$/DOL : DME = 1 : 1 (v/v)) (C: carbon).

organic electrolyte as long as the proportion of macropores (>50 nm) is negligible. Mesopores are responsible for achieving higher initial capacities by better transport of solvated electrolyte and lithium ions, but by themselves cannot sustain cycle life.[10,15,21] Cell cathodes containing porous carbon from carbonized ZIF-8 and solvo-MOF-5 show a marked improvement in cycling behaviour in comparison with the uncarbonized version, achieving stable capacities at 332.3 and 219.2 mA h g^{-1} over 40 cycles, despite starting with relatively moderate initial capacities. Their scaffold carbons are the least porous structures and are dominated by the presence of micropores with insufficient fractions of the mesopores that are essential for the electrolyte and ion mobilities that lead to higher initial capacities. The presence of large macropores are usually responsible for loss of capacity with cycling. Thus, batteries based on carbon from solvo-MOF-5 with 0.13 $cm^3\ g^{-1}$ of macropores show greater loss in capacity than carbon from ZIF-8 with negligible macropores, although the latter starts off with a lower initial capacity. The total pore volume of 1.92 $cm^3\ g^{-1}$ is much higher in carbon from RT-MOF-5 based cathodes, with 73% of pores present as mesopores giving rise to a high initial capacity at 1294.1 mA h g^{-1}. Most of the remaining pores are made up of micropores with negligible macropores; thus, this battery has shown excellent cycle stability, achieving 592.1 mA h g^{-1} over 40 cycles. The carbon from ZnFumarate shows the highest pore volume of the 4 carbonized samples at 3.99 $cm^3\ g^{-1}$, and with a very high concentration of mesopores at 2.24 $cm^3\ g^{-1}$, predictably forms cells with a higher initial discharge capacity at 1471.8 mA h g^{-1} (about 88% of the theoretical capacity) as compared with all other scaffolds. Since the micropore concentration is also large at 1.27 $cm^3\ g^{-1}$, stability in cycle life is also observed, as expected. However the concentration of macropores at 0.22 $cm^3\ g^{-1}$ leads to some capacity loss during longer cycling. Over the first 40 cycles the capacity is still impressive at 662.3 mA h g^{-1}; however, it shows a small downward trend, especially when compared with the very stable value for cells based on carbon from RT-MOF with negligible macropores.

In summary, variable hierarchically porous carbons were synthesized from direct carbonization of 4 different MOF precursors. The carbons have been evaluated as the cathode scaffolds in lithium–sulphur batteries. We have shown the impact of pore volume and pore size distribution of the carbonized MOFs loaded with sulphur on the capacity and the cycle life of Li–S batteries. In future work it should be possible to develop carbon materials with an optimum hierarchically porous structure with both mesoporosity and microporosity for good sulphur loading and electrochemical utilization.

The authors thank the Cambridge Overseas Trust (KX and SC) and the ERC (SC and AKC) for financial support.

References

1 C. N. R. Rao, A. K. Cheetham and A. Thirumurugan, *J. Phys.: Condens. Matter*, 2008, **20**, 083202.
2 S. J. Yang, T. Kim, J. H. Im, Y. S. Kim, K. Lee, H. Jung and C. R. Park, *Chem. Mater.*, 2012, **24**, 464–470.
3 W. Li and D. Y. Zhao, *Chem. Commun.*, 2013, **49**, 943–946.
4 P. G. Bruce, S. A. Freunberger, L. J. Hardwick and J.-M. Tarascon, *Nat. Mater.*, 2012, **11**, 19–29.
5 R. D. Rauh, K. M. Abraham, G. F. Pearson, J. K. Surprenant and S. B. Brummer, *J. Electrochem. Soc.*, 1979, **126**, 523–527.
6 D. Marmorstein, T. H. Yu, K. A. Striebel, F. R. McLarnon, J. Hou and E. J. Cairns, *J. Power Sources*, 2000, **89**, 219–226.
7 B. Scrosati, J. Hassoun and Y.-K. Sun, *Energy Environ. Sci.*, 2011, **4**, 3287–3295.
8 Y. V. Mikhaylik and J. R. Akridge, *J. Electrochem. Soc.*, 2004, **151**, A1969–A1976.
9 N. Jayaprakash, J. Shen, S. S. Moganty, A. Corona and L. A. Archer, *Angew. Chem., Int. Ed.*, 2011, **50**, 5904–5908.
10 X. Ji, K. T. Lee and L. F. Nazar, *Nat. Mater.*, 2009, **8**, 500–506.
11 B. Zhang, X. Qin, G. R. Li and X. P. Gao, *Energy Environ. Sci.*, 2010, **3**, 1531–1537.
12 C. Zhang, H. B. Wu, C. Yuan, Z. Guo and X. W. Lou, *Angew. Chem., Int. Ed.*, 2012, **51**, 9592–9595.
13 X. Liang, Y. Liu, Z. Wen, L. Huang, X. Wang and H. Zhang, *J. Power Sources*, 2011, **196**, 6951–6955.
14 R. Demir-Cakan, M. Morcrette, F. Nouar, C. Davoisne, T. Devic, D. Gonbeau, R. Dominko, C. Serre, G. Férey and J. M. Tarascon, *J. Am. Chem. Soc.*, 2011, **133**, 16154–16160.
15 X. L. Ji, S. Evers, R. Black and L. F. Nazar, *Nat. Commun.*, 2011, **2**, 325.
16 S. Lim, K. Suh, Y. Kim, M. Yoon, H. Park, D. N. Dybtsev and K. Kim, *Chem. Commun.*, 2012, **48**, 7447–7449.
17 W. Chaikittisilp, M. Hu, H. Wang, H.-S. Huang, T. Fujita, K. C. W. Wu, L.-C. Chen, Y. Yamauchi and K. Ariga, *Chem. Commun.*, 2012, **48**, 7259–7261.
18 K. S. Park, Z. Ni, A. P. Cote, J. Y. Choi, R. D. Huang, F. J. Uribe-Romo, H. K. Chae, M. O'Keeffe and O. M. Yaghi, *Proc. Natl. Acad. Sci. U. S. A.*, 2006, **103**, 10186–10191.
19 D. J. Tranchemontagne, J. R. Hunt and O. M. Yaghi, *Tetrahedron*, 2008, **64**, 8553–8557.
20 H. Li, M. Eddaoudi, M. O'Keeffe and O. M. Yaghi, *Nature*, 1999, **402**, 276–279.
21 G. Liu, Z. Su, S. Sarfraz, K. Xi and C. Lai, *Mater. Lett.*, 2012, **84**, 143–146.

